Remote sensing-derived spectral vegetation indices and forest carbon: testing the validity of models in mountainous terrain covered with high biodiversity

Pradeep Kumar[1,*] and M. K. Ghose[2]

[1]Forests, Environment and Wildlife Management Department, Government of Sikkim, Gangtok 737 102, India
[2]Sikkim Manipal University, Gangtok 737 102, India

Sequestration of carbon through forests is an important aspect in global climate change mitigation. Assessment of carbon in forests using remote sensing and GIS tools is one of the most important aspects of rapid and verifiable methodologies. A number of studies have shown the utility of spectral (vegetation) indices like NDVI in the assessment of forest carbon. However, there are limitations to this approach. The mountainous topography and high biodiversity affect the spectral values in pixels in multiple ways. The present article aims to test the validity of use of vegetation indices in high-biodiversity forests in mountains by modelling the ground based forest carbon measurement with vegetation indices of NDVI, EVI, SAVI and MSAVI in a multi-sensor, multi-season data environment with multiple regression methods like linear, power, logarithmic, polynomial and exponential. It is found that all the regressions have a poor coefficient of determination not even exceeding 0.2. It is concluded that the remote sensing-based spectral vegetation indices alone cannot be a proxy for forest carbon calculators in high biodiversity mountain forests.

Keywords: Biodiversity, forest carbon, mountain, remote sensing, vegetation indices.

WITH the forests being increasingly seen as a significant tool against climate change due their ability to act as a global carbon sink, there is a need for rapid but verifiable methodologies to assess the climate mitigation potential of forests. There may be disagreement at times over the so-called clean technologies like nuclear power, but mitigation through forestry is universally the most acceptable method. The multi-functionality of forests extends far beyond just mitigation. It offers a number of other ecosystem services ranging from biodiversity to catchment-area enrichment.

In the presence of chlorophyll, CO_2 from the atmosphere and water gets converted to sugars by using energy from sunlight during the process of photosynthesis. The internal metabolism of the tree consumes about half the sugars and the remaining half is used for building of wood, roots and leaves. This constitutes the biomass of the tree. About half of this biomass is carbon content of the tree[1]. The sheer complexity of processes of carbon capture through photosynthesis by the trees and the geographical spread of forests on the land makes the assessment of carbon captured by the forests quite challenging. The big geographical extent makes it almost economically impossible to survey the forests repetitively through the physical counting of trees and then assessing the carbon captured. Remote sensing offers a viable solution. According to the Food and Agricultural Organization (FAO) of the United Nations, there is need for forest inventory agencies and remote sensing agencies to work together so that up-scaling and validation of remote sensing products could be done[2]. In the past several studies have been done on modelling the spectral ratios like normalized difference vegetation index (NDVI), enhanced vegetation index (EVI) and soil adjusted vegetation index (SAVI), etc. to the forest carbon. However, in case of high biodiversity forests, the very mechanism of satellite remote sensing is expected to be encountered with challenges when it comes to carbon assessment, primarily because of contamination of pixels due to the capturing of reflectance from different tree species and storing it as a uniform value in a single pixel.

This article examines the usefulness of optical remote sensing-based spectral vegetation indices from moderate-resolution sensors in assessing the forest carbon in a high biodiversity mountain forest. For the purpose of evaluation of the validity of relationship with spectral bands/ratios, the biodiversity hotspot area in Eastern Himalaya, i.e. Sikkim, India has been selected.

Objectives

The reflectance from high diversity of species results in the contamination of remote sensing image pixels. The

*For correspondence. (e-mail: pradeepifs@gmail.com)

mountainous terrain also induces its own distortions. This may have an influence on the relationship between the spectral values and biophysical parameters of forests.

The aim of the present study is to find out whether the correlation between the remote sensing image-derived 'vegetation indices' and the biophysical parameter of 'forest carbon' holds good for forests with high tree species diversity in mountainous. If yes, what is the extent of such correlation?

Material and methods

Study site

Sikkim is a mountainous state of India in the Eastern Himalaya extending approximately 114 km from north to south and 64 km from east to west, between 27°00′46″–28°07′48″N lat. and 88°00′58″–88°55′25″E long. (Figure 1). It encompasses a great altitudinal compression ranging from 300 to 8585 m amsl. Sikkim is globally renowned for its biological diversity and is part of the Himalayan global biodiversity hotspot. The unique terrain, climate and biogeography of the state have resulted in the sustenance of varied eco-zones in close proximity. Sikkim has an area of 7096 sq. km. It covers just 0.2% of the geographical area of India, but has 26% of the country's total biodiversity. Species-wise, the state harbours over 5500 flowering plants, 557 orchids, 41 rhododendrons, 16 conifers, 28 bamboos, 362 ferns and its allies, 9 tree ferns, 30 primulas, 11 oaks and 1022 medicinal plants[3]. Forestry is the major land use in the state covering around 47.80% of the total geographical area[4]. Due to great altitudinal compression, the forests of Sikkim exhibit tremendous biological diversity. A summary of the forests of Sikkim is as follows.

Figure 1. Location of the study site, Sikkim.

Tropical moist deciduous forests

These types of forests are mainly confined to the foothill regions up to an elevation of 900 m with sal (*Shorea robusta*) as the main species along with a few deciduous components. In some places, chir pine (*Pinus roxburghii*) is present with the sal forest. The common species are *S. robusta*, *Tectona grandis*, *Alstonia scholaris*, *Bombax ceiba*, *Lagerstroemia parviflora* and *Terminalia myriocarpa*.

Tropical, subtropical dry evergreen and broad-leaved hill forests

The main tree species are *Macaranga denticulata*, *Schima wallichii*, *Eugenia* sp., *Castanopsis* sp., *Alnus nepalensis*, *Emblica officinalis*, *Mallotus philippensis*, *Adhatoda zeylancia*, *Beaumontia grandiflora* and *Bauhinia vahlii*, etc.

Montane moist temperate forests

The vegetation gradually changes from subtropical to sub-temperate in the altitudinal range 1800–2400 m, beyond which the vegetation becomes that of distinct temperate forest. In this region the dominant species are *Tsuga* (*hemlock*), *Acer*, *Michelia*, *Juglans*, associated with *Rosa*, *Rubus*, *Berberis* and *Viburnum*. Typical temperate forests like *Quercus* (oak), *Acer*, *Populus*, *Larix* and *Abies densa* dominate the region between 2400 and 2700 m.

Sub-alpine and dry temperate forests

The tree species of *Rhododendron* are found predominantly mixed with a variety of species like *Gaultheria*, *Euonymus*, *Viburnum*, *Juniperus*, *Lyonia*, *Pieris*, *Lycesteria*, *Lonicera*, *Rosa*, *Eurya*, *Symplocos* and *Rubus.*

Alpine forests

Moist alpine forests: The vegetation in this zone mainly comprises typical alpine meadows where tree growth is

completely arrested. Quite a few stunted bushy growth species of *Rhododendron* mixed with tough clumps of *Juniperus*, *Salix*, *Barberis*, *Rosa* and *Lonicera* are common.

Dry alpine: The vegetation is practically of scattered scrubs, often barren. Most of the species are of stunted thorny scrubs in nature. Some of the common species are *Berberis*, *Juniperus* and *Salix*.

Methodology

Study design and data collection

For establishing the correlation between actual field-based carbon and the image parameters, we laid the actual ground sample plots of 0.1 ha (31.61 m × 31.61 m) during 2009–10. Sample plot size of 0.1 ha was selected as this is the standard which has been worked upon and adopted by the Forest Survey of India (FSI) for the whole of India. This size was also adopted with the aim of future/past comparison of results with similar kinds of studies done in India. We measured girth at breast height (1.37 m) for tree species falling within the plot. On slopes the observations were taken from the elevated side. We planned a cluster of four such plots at every site so that the carbon values of the trees in these plots could be averaged in case there is a need to minimize locational registration errors of such plots in the image or to hierarchically model the values in a bigger pixel. For clustering these plots, we identified the grids of 250 m × 250 m prior to field work. We did the first-level stratification of the site on the basis of NDVI values. The whole area of Sikkim was divided into seven strata based on NDVI map prepared on the basis of satellite imagery. The NDVI slices (ranges) considered for different strata had values 0.1–0.2, 0, 2–0.3, 0.3–0.4, 0.4–0.5, 0.5–0.6 and 0.6 to >0.7. Based on the extent of area covered by different NDVI ranges, the proportionate number of plots was randomly selected in the areas with corresponding NDVI ranges. A total of 55 sites were selected based on the physical and financial constraints. The coordinates of the centre of the site were obtained from the map. To locate the site on the ground we used handheld global positioning system (GPS). We divided the site into four quadrates (NE, SE, SW and NW), and laid the four sample plots, about 75–90 m away from centre in each quadrat (Figure 2).

Sikkim has four districts, namely East Sikkim, West Sikkim, South Sikkim and North Sikkim. We selected 7 sites in East Sikkim, 9 in South Sikkim, 10 in West Sikkim and 29 in North Sikkim, thus making 55 sites. Each site had a cluster of four plots. Figure 3 shows the distribution of sites for plot clusters. In few sites some plots could not be laid due to inaccessibility. A total of 207 plots were laid. The total trees measured were 1088 in East Sikkim, 1526 in South Sikkim, 9321 in West Sikkim and 6063 in North Sikkim. Due to massive manpower requirements, manual rechecking of the plots in the difficult mountainous terrain was not possible. As a first-level

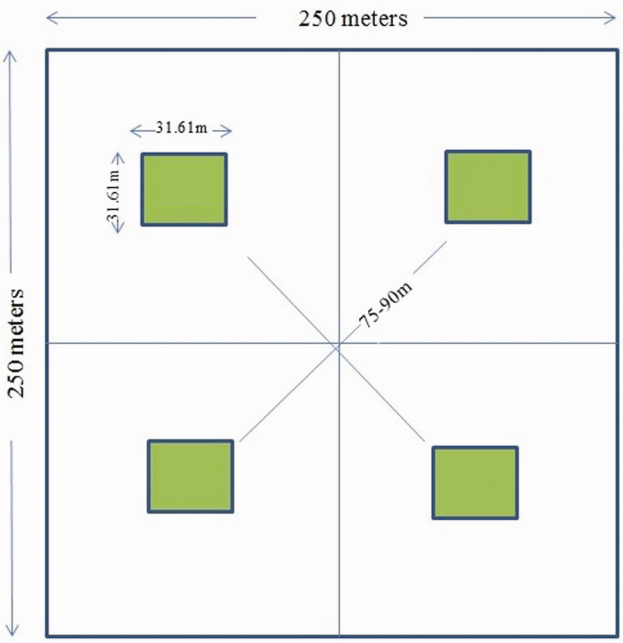

Figure 2. Layout of sample plots.

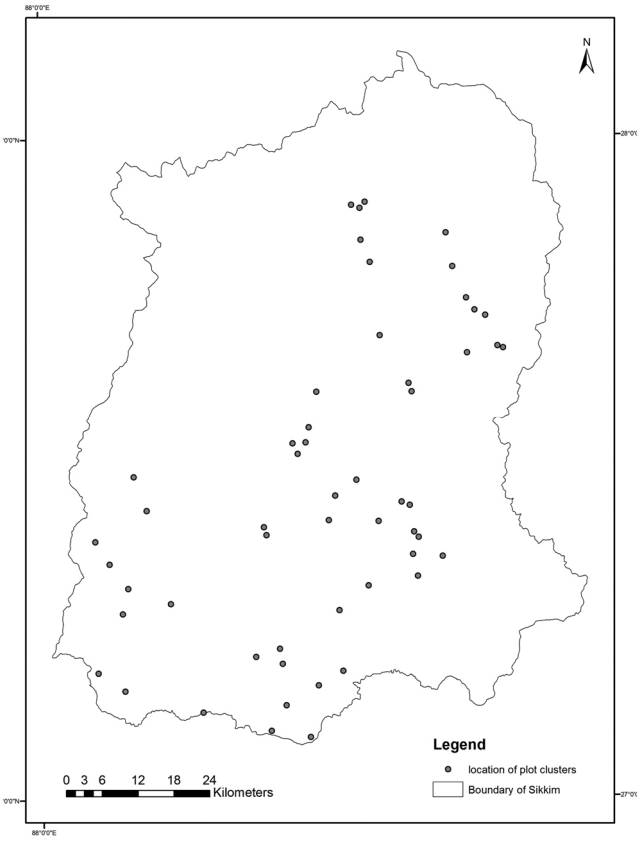

Figure 3. Location of plot clusters.

check on the data, we converted all the GPS locations of plots to kml file format and overlaid them on Google Earth. This helped in visualizing the locations of the plots. Some of the plots which seemed to be totally far away from other plots of the cluster were not taken into consideration for further calculations. This could have been due to incorrect GPS recording. Also, we did not take into account data from some plots due to certain issues with them, or the presence of some abnormally big tree in the plot which had the potential to disturb the expected most probable relationship. Finally, we used data from 44 sites spread over 171 plots.

Estimation of plot biomass and carbon

We processed the ground data thus collected for estimating biomass and carbon. We considered only the above-ground tree biomass for carbon estimation of the trees. This included the components of woody biomass and leaf biomass of all trees (i.e. all diameter classes). For biomass calculation, the trees were grouped into two classes – one with diameter 10 cm and above, and the other with diameter below 10 cm. The woody volume of trees for each sample plot was calculated using site-specific volume equations developed by FSI. This volume equation provides volume of main stem measured up to 10 cm diameter and volume of all branches having diameter 5 cm or more. Biomass was obtained by multiplying wood volume with specific gravity. For above-ground biomass of branches and foliage of trees having dbh $\geq$ 10 cm and above-ground biomass of trees having dbh < 10 cm, specially developed biomass equations were used[5]. The carbon content in the tree was obtained by multiplying the biomass with percentage carbon content of the species. The data of specific gravity and percentage carbon content for the trees were obtained from the literature. The data were processed in a specially prepared software package which took into account different species of trees, species-specific volume equation, above-ground biomass of branches and foliage of trees and data on specific gravity and percentage carbon content of most of the tree species from the literature. For a few species percentage carbon content was ascertained by experimentation and for others the average of all other species was used in the package. The field data collection was mostly in local names of the species. These local names were then converted to botanical names. Wherever the species could not be identified, the general volume equation was used.

Since the satellite imageries are two-dimensional and represent the areas on slopes of the mountains on a projected horizontal surface, the corresponding area on the imagery was equivalent to the plot area measured on the surface of slope multiplied by the tangent of the slope angle. Accordingly, the carbon density (tonnes of carbon per hectare) in the imagery was corrected. The carbon density represented in the imagery is more than the carbon density on the actual sloping area of the plot. We performed the slope correction of carbon thus obtained on the sloping surface by projecting it on the horizontal surface based on the slope of the area. This was basically obtained by dividing the carbon density as on the plot by the tangent of the angle of the slope.

Spectral ratios

The study site of Sikkim is completely mountainous terrain. This gives rise to the varying illumination conditions for different slopes. Similar vegetation may have different digital number (DN) values on different slopes depending upon the illumination conditions or the slope being in sunlit area or shadow area. However, this can be compensated by use of spectral ratios. At the same time, the spectral ratios are useful in capturing the material-specific (like vegetation) variations in reflectance over different bands. It basically involves the mathematical division of a pixel in one band by the corresponding pixel in other band. Studies[6–8] have shown that the relationship between the energy reflected in the red and infrared (IR) bands is dependent on the amount of vegetation present on the ground. Depending upon the leaf area index, morphologies of leaves and leaf angle distribution, very little near-infrared (NIR) radiation is absorbed and therefore most of the NIR radiation is scattered through reflectance and transmittance. Consequently, the contrast between the responses in red and NIR bands becomes a sensitive measure of the amount of vegetation[9]. Vegetation ratios in red and IR bands are a good measure of vegetation activity. The advantage of ratioing is that these ratios enhance the vegetation signal from the spectral responses. Some of the vegetation ratios used in the present article are as follows[10].

Normalized difference vegetation index (NDVI)

NDVI is calculated by dividing the difference between near infrared and red (R) values by the sum of R and NIR values

$$\mathrm{NDVI} = \frac{\mathrm{NIR} - \mathrm{R}}{\mathrm{NIR} + \mathrm{R}}.$$

Values of NDVI range from –1 to +1.

Soil adjusted vegetation index (SAVI)

SAVI uses the R and NIR values for ratioing. Here a soil brightness correction factor (L) is applied. L has been defined as 0.5 to accommodate most land-cover types

$$\mathrm{SAVI} = \left(\frac{\mathrm{NIR} - \mathrm{R}}{\mathrm{NIR} + \mathrm{R} + \mathrm{L}}\right) \times (1 + L).$$

Enhanced vegetation index (EVI)

EVI has the ability to decouple the canopy background signal and reduce the atmosphere influences. It has improved sensitivity over high biomass regions[11]

$$\mathrm{EVI} = \frac{\mathrm{NIR} - \mathrm{R}}{\mathrm{NIR} + C1 * \mathrm{R} - C2 * B + L},$$

where L is the canopy adjustment factor, C the coefficients for atmospheric resistance and B represents values from the blue band.

Modified soil adjusted vegetation index (MSAVI)

MSAVI also uses the R and NIR values for ratioing but to reduce the soil effects on reflectance from the vegetation to its maximum, an inductive function is applied.

MSAVI is calculated as follows

$$\mathrm{MSAVI} = (2 * \mathrm{NIR} + 1 - \sqrt{((2 * \mathrm{NIR} + 1)^2 - 8 * (\mathrm{NIR} - \mathrm{R}))})/2.$$

Image acquisition

We downloaded the moderate resolution imaging spectroradiometer (MODIS) surface reflectance-derived products of vegetation indices for January 2009, March 2009, November 2009, April 2009 and December 2010.

For Landsat, data availability for the relevant period was from that of Landsat 7, but all were Landsat 7 ETM + SLC-off data when the scan line corrector (SLC) had failed. These products have data gaps. Landsat 7 ETM + SLC-off inputs acquired after 31 May 2003 are not gap-filled in spectral indices production. We downloaded only one image of March 2009, but it was not of much use due to data gaps in the form of strips. For Landsat, we used the Landsat8 data of November 2013 even though there is a gap of four years. We presumed that the vegetation indices may have changed from 2009 to 2013, but the empirical relationship, if any, between the vegetation indices and biomass would not have changed significantly.

Since the pixel size of Landsat (~30 m × 30 m) was almost close to the size of the individual sample plot (0.1 ha), we used the single corresponding sample plot for studying the relationship of carbon in the plot to the vegetation indices of the Landsat pixel. We calculated per pixel carbon by multiplying the pixel area (ha) with carbon density (tonnes/ha). We obtained the carbon density for the pixel by dividing the carbon in the respective sample plot by the area of the sample plot.

We used handheld global positioning system (GPS) for recording the locations of the plots. There could be the possibility of poor registration of GPS location of sample plot with the corresponding pixel. To minimize the error on this account, we took the usable cluster of ground plots falling in the MODIS pixel (250m_16_days_composite_day_of_the_year), and averaged the carbon value for the area of MODIS pixel. We established the correlations between vegetation indices and forest carbon. We obtained the quality of pixels by extracting the quality at the respective locations from the MODIS 250m_16_days_VI_Quality file. We obtained the pixel reliability by extracting the reliability codes at the respective locations from the MOD13Q1.A2010337.250m_16_days_pixel_reliability file. We only used pixels with good reliability (code 0 pertaining to reliability category 'Good', where data can be used with confidence, and code 1 pertaining to reliability category 'Marginal' where data are useful, but referring to other QA information is advised).

Data analysis – regression of field plot data against vegetation indices

In case of Landsat images, we obtained the following 30 m Landsat surface reflectance-derived spectral indices products: NDVI, EVI, SAVI and MSAVI.

We calculated the carbon in one pixel by multiplying the unit pixel area (i.e. 0.09 ha) with the carbon density (tonnes/ha). We had already obtained the carbon density for the pixel by mathematically dividing the carbon in the respective sample plot by the area of the sample plot (0.1 ha).

We extracted values of all the above vegetation indices at the respective GPS locations in ArcGIS 10.3. We tabulated these locations against the carbon values of the respective pixels and regressed them with exponential, linear, logarithmic, polynomial and power regression types.

In case of MODIS images, we used MOD13Q1 (16-day 250 m) VI product, which is generated using the daily MODIS Level-2G (L2G) surface reflectance. We used two indices, NDVI and EVI. Here too, we calculated the carbon in one pixel by multiplying the unit pixel area of MODIS with the carbon density (tonnes/ha). Carbon density for the pixel was obtained by dividing the carbon in the respective sample plot by the area of the sample plot. We filtered these locations in the second stage by the quality and reliability. We then tabulated filtered locations against the carbon values of the respective pixels and regressed with exponential, linear, logarithmic, polynomial and power regression types.

Results and discussion

Saturation of signals at high biomass is a well-known and well-documented phenomenon[12–14]. However, in the

present study additional issues were observed. The scatter plots between vegetation indices and forest carbon showed not only the saturation of signal at high carbon values, but also lacked any significant trend even at lower carbon values. This leaves the vegetation indices with limited applicability in forest carbon assessment in high biodiversity mountain forests. The scatter plots have been drawn for all the combinations of sensor, vegetation indices and regression types. Among these, only some representative scatter plots are given here (Figures 4–6). It can be observed from these scatter plots that it is difficult to observe any significant correlation between any type of vegetation index and forest carbon in high biodiversity mountains.

The study was aimed at exploring the applicability of vegetation indices as the main variable in forest carbon assessment. In order to examine the possibility of correlation of forest carbon solely with vegetation indices across the complete spectrum, a whole range of sample plots

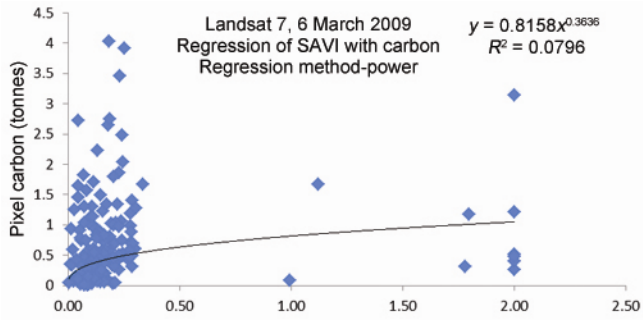

Figure 4. Regression of SAVI with pixel carbon.

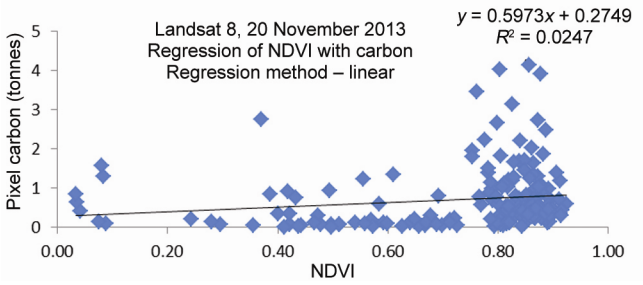

Figure 5. Regression of NDVI with pixel carbon.

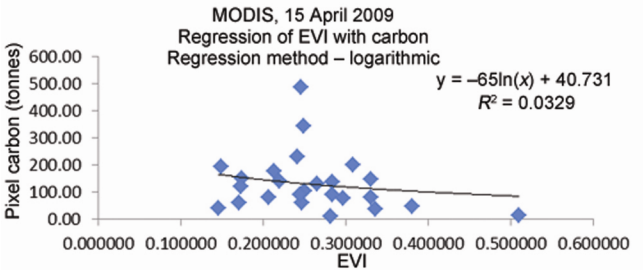

Figure 6. Regression of EVI with pixel carbon.

(data points) representing both low and high carbon values, different forest types, multiple density classes and different altitudinal ranges was taken into account for regression between vegetation indices and carbon values. In other words, the only independent variable considered in the study was vegetation index, and it was presumed that the all other factors which might affect the forest carbon will be subsumed in the vegetation index. The selective range of other variables (like forest density and altitudes) was not considered to exclude the possibility of any chance correlation, when the regression is performed in the limited regression environment within a limited range of altitude or forest type.

Several studies have shown that NDVI could be a good predictor of forest carbon at low forest carbon values[15,16]. Contrary to this conclusion, Table 1 shows the result of regression from the study area in the form of coefficient of determination (R^2). It is evident from the table that very high number of species contained in a single pixel and different mix of species in different pixels in mountainous terrain contaminate the pixel to an extent that renders it unusable for calibrating vegetation indices with biomass or carbon.

This pixel contamination could have occurred as the relationship between the spectral response measured by the sensor and forest carbon (biomass) is dependent on the optical properties of forests like canopy geometry and leaf spectral properties[17]. These parameters are directly affected by biodiversity. At the same time the relationship between spectral response measured by the sensor and forest carbon (biomass) is also dependent on system factors such as topography, sun elevation, haze, wind speed and orientation and inclination of the view axis between the surface and the sensor which are directly affected by the terrain[17].

In an area with a diverse mix of species where there is high biodiversity within a single patch and also the mix of species changes in the different patches (i.e. a high Shannon index coupled with low Sorenson's coefficient), any inference on carbon drawn on the basis of just the vegetation indices will not be credible, at least with these moderate-resolution optical sensors like MODIS and Landsat; therefore remote sensing-based spectral vegetation indices alone cannot be the proxy for carbon calculators in such high biodiversity forests.

It is apparent that the high biodiversity-induced spectral response could be one of the prime disrupters in achieving a coherent relationship between vegetation indices and forest carbon. If the spectral response itself could capture the types and patterns of biodiversity, the biodiversity-induced pixel contamination could be offset by some algorithm, or alternatively, the level of pixel contamination could also be another variable along with vegetation indices for assessment of forest carbon. This is possible if the species diversity could be integrated in spectral response during remote sensing. However, the

Table 1. Regression of vegetation indices with pixel carbon

Season/date	Sensor	Vegetation index/band	Coefficient of determination (R^2) regression method				
			Exponential	Linear	Log	Polynomial	Power
1 January 2009	MODIS	EVI	0.0073	0.0128	0.0175	0.0238	0.0071
		NDVI	0.1519	0.1446	0.1269	0.1736	0.1294
22 March 2009	MODIS	EVI	0.1649	0.133	0.1273	0.1338	0.1551
		NDVI	0.0187	0.0056	0.0168	0.0482	0.0351
7 April 2009	MODIS	EVI	0.0223	2.00E-06	0.0008	0.0172	0.0246
		NDVI	0.1156	0.0372	0.0463	0.0545	0.1495
15 April 2009	MODIS	EVI	0.1743	0.0581	0.0329	0.1029	0.113
		NDVI	0.002	7.00E-05	0.0021	0.1047	0.00002
9 November 2009	MODIS	EVI	0.0073	0.0128	0.0175	0.0238	0.0071
		NDVI	0.1519	0.1446	0.1269	0.1736	0.1294
3 December 10	MODIS	EVI	0.0675	0.0023	0.0083	0.0364	0.0941
		NDVI	0.2701	0.1426	0.1387	0.1426	0.2587
20 November 13	Landsat 8	EVI	0.084	0.0093	0.02	0.0382	0.0998
		NDVI	0.0857	0.0247	0.0088	0.0415	0.0214
		SAVI	0.0832	0.0108	0.0178	0.0309	0.0776
		MSAVI	0.0772	0.0079	0.0183	0.0183	0.0878
6 March 2009	Landsat 7	EVI	0.0154	0.01	0.0413	0.0248	0.0792
		NDVI	0.0565	0.0435	0.0526	0.085	0.0785
		SAVI	0.0245	0.0163	0.0471	0.0543	0.0796
		MSAVI	0.0216	0.0143	0.0469	0.0472	0.0803

estimation of relationships between the spectral values and species distributions is useful for a limited purpose and subject to substantial errors[18,19]. Therefore, with the current state of knowledge, the removal of pixel contamination due to biodiversity or the integration of species diversity in vegetation index cannot be reliably done.

Data synergy or fusion, i.e. the mechanism whereby discrete types of data are used together to achieve a better understanding than is possible with each individually[20], may not be of much use in this case, where primary data of remote sensing pixel are contaminated. However, this should not be taken to indicate that moderate resolution optical remote sensing has no utility in high biodiversity mountainous areas for carbon assessment. Given the physical and financial resources involved in surveying, remote sensing is the only answer. While using a suite of other available methods in flat terrains with low biodiversity, products like Landsat-8 seem best suited for broader spatial-scale forest carbon products, while airborne lidar can be used for estimating fine-scale above-ground forest carbon mapping with low uncertainty[21]. Vegetation index-based calibrations of carbon in high biodiversity mountain forests will be subject to large errors. This calls for alternatives like using remote sensing for forest density mapping and for classifying the various types in combination with other tools and data. Carbon density (i.e. carbon in tonnes per hectare) of different typical forest type–density combination classes can be estimated. Based on the area (ha) in these classes and the carbon density therein, the carbon content in a particular forest can be calculated. Remote sensing is one of the best tools for preliminary stratification on a broader scale. Stratification can improve the predictive accuracy[22], where some acceptable correlation between remote sensing-derived parameter and forest carbon can be obtained. Simultaneously there can be other pathways to arrive at the desired result. They can also include various other forms of remote sensing, like lidar, hyperspectral and microwave remote sensing, either as standalone or in combination depending upon their usability, availability and accuracy.

1. McKinley, D. C. *et al.*, A synthesis of current knowledge on forests and carbon storage in the United States. *Ecol. Appl.*, 2011, **21**, 1902–1924.
2. FAO, *Biomass, Assessment of the Status of the Development of the Standards for the Terrestrial Essential Climate Variables*, Food and Agriculture Organization, Rome, Italy, 2006.
3. Envis Centre, Sikkim; http://www.sikenvis.nic.in/Database/Biodiversity_776.aspx (accessed on 17 December 2015).
4. SFR, India State of Forest Report 2015, Forest Survey of India Dehradun, India, 2015.
5. Forest Survey of India, Carbon Stock in India's Forests.
6. Asrar, G., Fuchs, M., Kanemasu, E. T. and Hatfield, J. L., Estimating absorbed photosynthetic radiation and leaf area index from spectral reflectance in wheat. *Agron. J.*, 1984, **76**, 300–306.
7. Baret, F. and Guyot, G., Potentials and limits of vegetation indices for LAI and APAR assessment. *Remote Sensing Environ.*, 1991, **35**, 161–173.
8. Colwell, J. E., Vegetation canopy reflectance. *Remote Sensing Environ.*, 1974, **3**, 175–183.

9. Huete, A., Justice, C. and Leeuwen, W. van., MODIS Vegetation Index (Mod 13) Algorithm Theoretical Basis Document, Universty of Arizona, University of Virginia, 1999.
10. Masek, J. G. *et al.*, A landsat surface reflectance dataset for North America, 1990– 2000. *IEEE Geosci. Remote Sensing Lett.*, 2006, **3**, 68–72.
11. Solano, R., Didan, K., Jacobson, A. and Huete, A., MODIS vegetation index user's guide (MOD13 series). *Veg. Index Phenol. Lab.*, 2010.
12. Huete, A. *et al.*, Overview of the radiometric and biophysical performance of the MODIS vegetation indices. *Remote Sensing Environ.*, 2002, **83**, 195–213.
13. Lu, D., The potential and challenge of remote sensing-based biomass estimation. *Int. J. Remote Sensing*, 2006, **27**, 1297–1328.
14. Lu, D. *et al.*, A survey of remote sensing-based aboveground biomass estimation methods in forest ecosystems. *Int. J. Digit. Earth*, **9**, 2016, 63–105.
15. Goswami, S., Gamon, J., Vargas, S. and Tweedie, C., Relationships of NDVI, biomass, and leaf area index (LAI) for six key plant species in Barrow, Alaska, 2015; doi:10.7287/peerj.preprints.913v1.
16. Zhu, X. and Liu, D., Improving forest aboveground biomass estimation using seasonal Landsat NDVI time-series. *ISPRS J. Photogramm. Remote Sensing*, 2015, **102**, 222–231.
17. Wulder, M. A., Hall, R. J., Coops, N. C. and Franklin, S. E., High spatial resolution remotely sensed data for ecosystem characterization. *BioScience*, 2004, **54**, 511.
18. Kerr, J. T. and Ostrovsky, M., From space to species: ecological applications for remote sensing. *Trends Ecol. Evol.*, 2003, **18**, 299–305.
19. Nagendra, H., Using remote sensing to assess biodiversity. *Int. J. Remote Sensing*, 2001, **22**, 2377–2400.
20. Benson, M., Pierce, L. and Sarabandi, K., Estimating boreal forest canopy height and above ground biomass using multi-modal remote sensing; a database driven approach. in 2498–2501, IEEE, 2016; doi:10.1109/IGARSS.2016.7729645.
21. Wu, Z., Dye, D., Vogel, J. and Middleton, B., Estimating forest and woodland aboveground biomass using active and passive remote sensing. *Photogramm. Eng. Remote Sensing*, 2016, **82**, 271–281.
22. Latifi, H. *et al.*, Stratified aboveground forest biomass estimation by remote sensing data. *Int. J. Appl. Earth Obs. Geoinform.*, 2015, **38**, 229–241.

ACKNOWLEDGEMENT. We thank the Indian Institute of Remote Sensing, Dehradun for financial support, and the Forest Survey of India, Dehradun for help in processing the data.

Received 3 September 2016; revised accepted 28 December 2016

doi: 10.18520/cs/v112/i10/2043-2050